

# Effects of alloying elements on the Ni/Ni<sub>3</sub>Al interface strength and vacancy diffusion behavior

Cite as: J. Appl. Phys. **128**, 175307 (2020); <https://doi.org/10.1063/5.0028621>

Submitted: 06 September 2020 . Accepted: 13 October 2020 . Published Online: 05 November 2020

Qiuhao Wen, Mingxu Wang,  Lingti Kong, and  Hong Zhu



View Online



Export Citation



CrossMark

## ARTICLES YOU MAY BE INTERESTED IN

[Exploring benefits of composition grading for forward-IV characteristics of In<sub>1-x</sub>Ga<sub>x</sub>As LEDs for cryogenic applications](#)

Journal of Applied Physics **128**, 175701 (2020); <https://doi.org/10.1063/5.0013996>

[Two-dimensional WS<sub>2</sub> crystals at predetermined locations by anisotropic growth during atomic layer deposition](#)

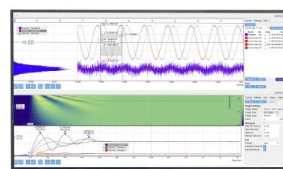
Journal of Applied Physics **128**, 175302 (2020); <https://doi.org/10.1063/5.0011249>

[Experimental demonstration of the wave attenuation capability of a piezoelectric metamaterial beam by using correlation for signal processing](#)

Journal of Applied Physics **128**, 174903 (2020); <https://doi.org/10.1063/5.0014742>

Challenge us.

What are your needs for periodic signal detection?



Zurich  
Instruments



# Effects of alloying elements on the Ni/Ni<sub>3</sub>Al interface strength and vacancy diffusion behavior

Cite as: J. Appl. Phys. 128, 175307 (2020); doi: 10.1063/5.0028621

Submitted: 6 September 2020 · Accepted: 13 October 2020 ·

Published Online: 5 November 2020



Qiu hao Wen,<sup>1</sup> Ming xu Wang,<sup>2</sup> Ling ti Kong,<sup>2,3</sup>  and Hong Zhu<sup>1,2,3,a)</sup> 

## AFFILIATIONS

<sup>1</sup>University of Michigan—Shanghai Jiao Tong University Joint Institute, Shanghai Jiao Tong University, Shanghai 200240, People's Republic of China

<sup>2</sup>School of Materials Science and Engineering, Shanghai Jiao Tong University, Shanghai 200240, People's Republic of China

<sup>3</sup>Materials Genome Initiative Center, Shanghai Jiao Tong University, Shanghai 200240, People's Republic of China

<sup>a)</sup>Author to whom correspondence should be addressed: [hong.zhu@sjtu.edu.cn](mailto:hong.zhu@sjtu.edu.cn)

## ABSTRACT

The effects of seven alloying elements (Co, Cr, Mo, Re, Ru, Ta, and W) on the Ni-vacancy diffusion behavior and the rupture strength of  $\gamma$ -Ni/ $\gamma'$ -Ni<sub>3</sub>Al interfaces are studied using density functional theory calculations. Our results reveal that all seven solutes prefer to occupy Al sites close to or Ni sites far from the interface. These solutes except for Co could significantly increase the barrier of Ni-vacancy diffusion within the  $\gamma/\gamma'$  interface region. The retarding effects are similar when solutes are located at their favored Al and Ni sites, which follows the sequence of Ta > W > Mo > Re > Ru > Cr > Co. Besides, it is found that the presence of solute atoms could always increase the rupture strength of their neighboring interface but reduce that of their next neighboring interface. The best strengthening effects on the neighboring interface are achieved by Re and W. In terms of the entire interface region, alloying at the favored Al site brings a better strengthening effect than that at the favored Ni site. The charge density difference analysis demonstrates that the charge accumulation level at the interface explains the variable strengthening effects among different alloying elements.

Published under license by AIP Publishing. <https://doi.org/10.1063/5.0028621>

## I. INTRODUCTION

Ni-based single-crystal superalloy is a very important class of engineering materials with an exceptional combination of high mechanical strength, good thermal creep resistance, and excellent corrosion resistance. They have wide applications in critical facilities, such as aircraft turbines, rocket engines, and nuclear power or chemical processing plants.<sup>1-3</sup>

However, the fluctuant force synergized with high service temperatures would still cause damages to superalloys. During service operation, superalloys may encounter failure because of the extensive creep deformations or even the creep rupture. To improve the service performance and to extend the service lifetime, various alloying elements are added into the Ni-based single-crystal superalloy for solid solution strengthening, which has been the main design strategy in the last decades.

It has been proved that the creep deformation of single-crystal superalloys is governed by the formation and migration of dislocations.<sup>4-9</sup> Meanwhile, some studies reveal that the dislocation

climbing process is controlled by the  $\gamma/\gamma'$  interface because it can interact with dislocations and hinder them from cutting into  $\gamma'$  precipitates.<sup>4,5,10-12</sup> Since the movement of dislocation relies on the motion of vacancy,<sup>4,13,14</sup> slower vacancy diffusion through the  $\gamma/\gamma'$  interface would contribute to a better creep deformation resistance. Besides, failure analyses of superalloys subjected to different stresses and temperatures have demonstrated that the  $\gamma/\gamma'$  interface is the weakest part in Ni-based single-crystal superalloys.<sup>1,15-17</sup> As a consequence, the rupture strength of the  $\gamma/\gamma'$  interface could represent the rupture strength of superalloys to a certain extent.

Since the  $\gamma/\gamma'$  interface plays such a critical role in controlling the creep deformation rate and creep rupture strength, obtaining an in-depth understanding of the interaction between solutes and  $\gamma/\gamma'$  interface becomes the prerequisite for designing new generation superalloys. Numerous investigations via theoretical and experimental approaches have been made to reveal these interactions. Sun *et al.*<sup>18,19</sup> studied the effect of Re on vacancy diffusion in the  $\gamma/\gamma'$  interface region. Their first-principles calculations reveal that Re atoms can inhibit both the formation and migration of

Ni-vacancy. Considering that Ni is the main constituent of superalloys, they suggest that Re doping could strongly reduce the diffusivity of vacancy throughout the interface and thereby increase the structural stability. Recently, Zhao *et al.*<sup>20</sup> did an exploratory study on the migration barrier of Ni-vacancy diffusion within the  $\gamma/\gamma'$  interface region alloyed with Re, Mo, and Ta, respectively. According to the calculation results, both Re and Mo increase the migration barriers of Ni-vacancy, while Re has a stronger hindering effect. Peng *et al.*<sup>16</sup> investigated the strengthening effects of Re on the  $\gamma/\gamma'$  interface region in terms of the Griffith work and found that their substitution for Ni at the coherent (002)  $\gamma/\gamma'$  atomic layer was beneficial for improving the rupture strength of the  $\gamma/\gamma'$  interface. Subsequently, Gong and Zhu *et al.*<sup>20–23</sup> performed studies on the effects of other metal alloying elements theoretically and experimentally. Their results showed that the addition of Co, Re, Ta, and W at their energetically favored Ni sites cannot increase the rupture strength of interface, while the substitutions at their favored Al sites improve the rupture strength of Ni-based single-crystal superalloy. Among them, the best strengthening effect is achieved by Re and W, while Ta appears to be less potent and Co has little effect.

Despite the prior works, a comprehensive understanding about the impacts of alloying elements within the  $\gamma$ -Ni/ $\gamma'$ -Ni<sub>3</sub>Al interface region is still missing. First, since there are more than 10 kinds of alloying elements added into the Ni-based single-crystal superalloy, more common elements in superalloys such as Co, Cr, Mo, and Ru<sup>4,24</sup> should be taken into consideration with respect to their effects on the Ni-vacancy diffusion behavior in the  $\gamma/\gamma'$  interface region. Second, as the coherent layer of  $\gamma$  phase and  $\gamma'$  phase, the atomic layer (002)  $\gamma/\gamma'$  can be regarded as either the surface of  $\gamma$  block or that of the  $\gamma'$  block. As a consequence, two potential fracture planes exist at the  $\gamma/\gamma'$  interface region.<sup>25</sup> However, most research studies<sup>20,21,23</sup> merely focus on the potential fracture plane between (002)  $\gamma/\gamma'$  and (001)  $\gamma'$ , probably because it is weaker than the plane between (002)  $\gamma/\gamma'$  and (001)  $\gamma$  when the system is free of solutes. However, alloying may change the situation. For example, Peng *et al.*<sup>16</sup> observed an inverse tendency after Re is doped at the (001)  $\gamma'$  atomic layer. Therefore, both the potential fracture planes should be taken into consideration to get a comprehensive understanding about the effects of solutes on the  $\gamma/\gamma'$  interface rupture strength.

In this work, the alloying of the most commonly used solute elements in Ni-based superalloys including Co, Cr, Mo, Re, Ru, Ta, and W is systematically studied by first-principles calculations. The diffusion behavior of Ni-vacancy around solutes is investigated using the climbing image nudged elastic band (CI-NEB) method. Besides, their effects on the rupture strength of both potential fracture planes are evaluated by the Griffith work. Our research can provide a comprehensive and profound understanding of the alloying elements with respect to their effects on the property of the  $\gamma/\gamma'$  interface and further contribute to the development of superalloys with extended service lifetime.

## II. COMPUTATIONAL METHODS

A coherent  $\gamma$ -Ni/ $\gamma'$ -Ni<sub>3</sub>Al interfacial supercell is built under the guidance of experiments,<sup>26,27</sup> which contains 112 atoms with  $\gamma$ -Ni and  $\gamma'$ -Ni<sub>3</sub>Al each occupying seven atomic layers. After full

structure relaxation, a 10 Å vacuum is added along the [001] direction to avoid the interaction between adjacent interfaces, as shown in Fig. 1(a). Besides, the first atomic layer on each surface is fixed in all directions during calculations to reduce the influence of the vacuum layer.

The atomic layers  $-2$ ,  $1$ , and  $-1$  in Fig. 1(a) represent the (001) atomic layer in the  $\gamma$ -Ni block, the (001) atomic layer in the  $\gamma'$ -Ni<sub>3</sub>Al block, and the (002) coherent  $\gamma/\gamma'$  interfacial layer, respectively. Interface-I is the plane bounded by atomic layers  $1$  and  $-1$ , and interface-II is that bounded by atomic layers  $-1$  and  $-2$ . We define the middle four layers with the atomic layer number ranging from  $-2$  to  $2$  as the  $\gamma/\gamma'$  interface region. The representative sites in the  $\gamma/\gamma'$  interface region are labeled by atomic species and Arabic numbers. Each labeled site represents a set of equivalent sites within the same atomic layer.

The calculations in this work are all based on the density functional theory (DFT)<sup>28,29</sup> and carried out within the Vienna *ab initio* simulation package (VASP).<sup>30</sup> The projector augmented wave method<sup>31,32</sup> and the general gradient approximation in the Perdew–Burke–Ernzerhof form (GGA-PBE)<sup>33</sup> are used in the calculations. The CI-NEB<sup>34</sup> method implemented in the transition state tools for VASP (VTST)<sup>35</sup> is used to search the saddle point of the Ni-vacancy diffusion process and further evaluate the impact of alloying element. The cutoff energy of the wave functions is taken as 520 eV. The convergence criteria of energy and force are set to  $10^{-5}$  eV/atom and 0.01 eV/Å, respectively. Brillouin zone integrations are sampled on a  $5 \times 5 \times 1$  mesh for calculation after checking the convergence with respect to k-points.

## III. RESULTS AND DISCUSSION

### A. Site preferences of alloying elements at the $\gamma/\gamma'$ interface region

As we focus on the effects of alloying elements at the  $\gamma/\gamma'$  interface region and there are several nonequivalent sites, it is necessary to identify the favored substitutional sites for each solute first. The site preferences of alloying elements could be achieved based on the substitutional formation energy  $E_{sub}$ ,<sup>36,37</sup> which reflects the thermodynamic propensity of replacing a host atom with another solute atom in the system. The substitutional formation energy is defined as

$$E_{sub} = E_{\gamma/\gamma'}^X + \mu_{Al/Ni} - E_{\gamma/\gamma'}^{pure} - \mu_X, \quad (1)$$

where  $E_{\gamma/\gamma'}^X$  and  $E_{\gamma/\gamma'}^{pure}$  represent total energies of the model with and without solute  $X$  ( $X = \text{Co, Cr, Mo, Re, Ru, Ta, and W}$ ), respectively.  $\mu_{Al/Ni}$  is the chemical potential of Al or Ni atoms, and  $\mu_X$  is the chemical potential of solute atom  $X$ . Considering that  $\gamma'$ -Ni<sub>3</sub>Al is surrounded by  $\gamma$ -Ni and formed under Ni-rich conditions, we adopt the chemical potential of Ni from its pure bulk status, while Al is from the bulk Ni<sub>3</sub>Al. As for the alloying elements, their chemical potentials refer to the corresponding pure bulk substance.<sup>38</sup>  $E_{sub}$  for alloying elements at different sites are shown in Fig. 1(b), in which the horizontal axis corresponds to the substitution position described in Fig. 1(a).

As shown in Fig. 1(b), the site preferences in the  $\gamma/\gamma'$  interface region are given in a sequence of Al-1 > Ni-5 > Ni-4 > Ni-3 > Ni-1 > Ni-2 for nearly all solutes, except for Ru and Co, which

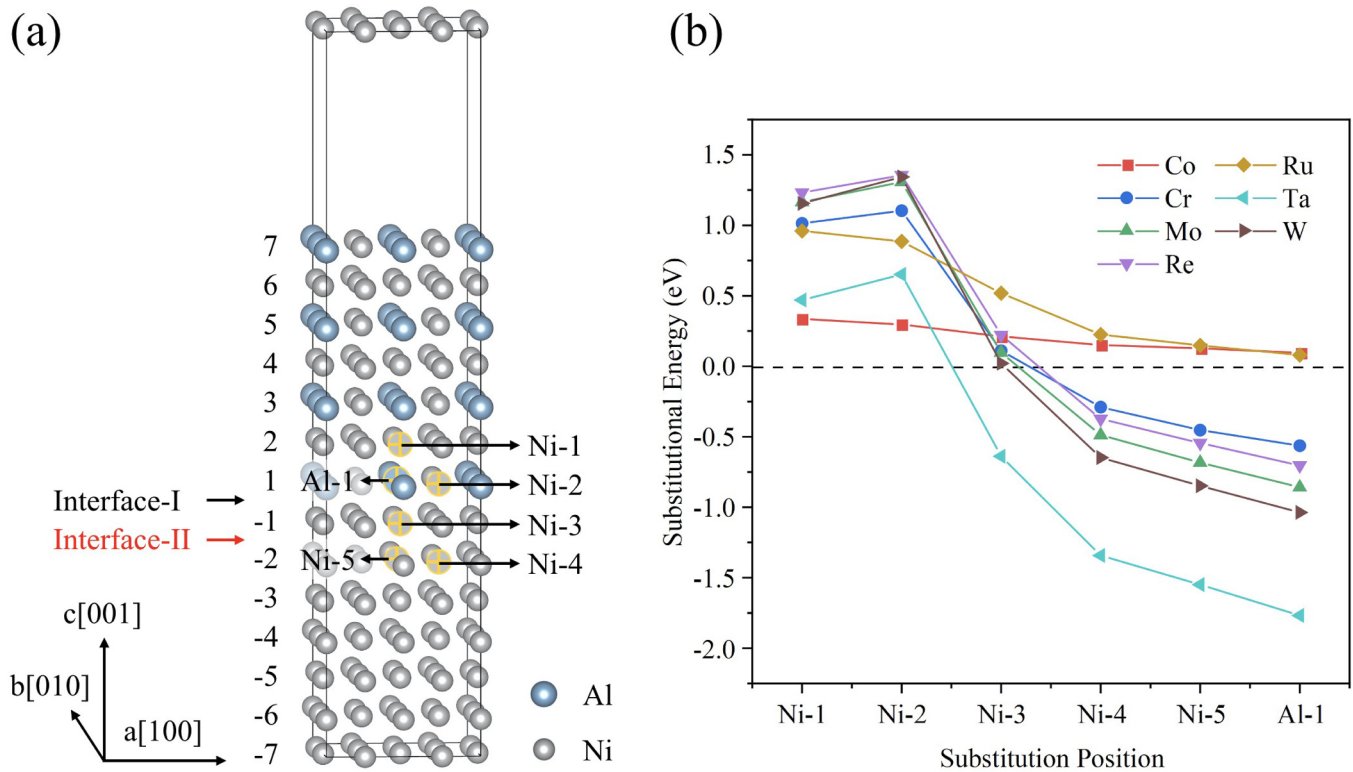


FIG. 1. (a) The construction of the  $\gamma$ -Ni/ $\gamma'$ -Ni<sub>3</sub>Al supercell model, with the representative atoms in each layer within the  $\gamma/\gamma'$  interface region labeled by atomic species and Arabic numbers. (b) The substitutional formation energies ( $E_{\text{sub}}$ ) of solute atoms at different representative sites in the  $\gamma/\gamma'$  interface region.

prefer Ni-2 over Ni-1. This sequence is almost the same as the previous work by Gong and Zhu *et al.*<sup>21,23</sup> Among the six representative sites in the  $\gamma/\gamma'$  interface region, the Al-1 site has the lowest substitutional energy regardless of the alloying element type, representing the most stable and favored substitutional site. Besides, all of these alloying elements have the second-lowest substitutional energy in the interface region at the Ni-5 site, which is the lowest among all Ni sites. This result indicates that these solute atoms prefer to replace the host atoms at the Al-1 site and the Ni-5 site most. Our results are also in line with the experimental studies.<sup>39–41</sup>

Moreover, we find that the stabilities of alloyed interfaces with different alloying elements vary a lot even for the same substitutional sites. For example, when these elements are doped at their favored Al-1 or Ni-5 sites, the stabilities of alloyed interfaces have a sequence as  $\text{Ta} > \text{W} > \text{Mo} > \text{Re} > \text{Cr} > \text{Co} \approx \text{Ru}$ . These results are basically consistent with Gong *et al.*<sup>21</sup>

## B. Alloying effects on Ni-vacancy diffusion

As we have introduced, the creep deformation of superalloys is governed by the dislocation movement around the  $\gamma/\gamma'$  interface region, which further relies on the diffusion of vacancies.<sup>13,20</sup> Therefore, studying the effect of solutes on vacancy diffusion is

important for us to further understand their influence on the creep deformation process of superalloys. The diffusion process in superalloys obeys the monovacancy mechanism which involves two steps, vacancy formation and vacancy-atom exchange.<sup>42–45</sup> The former step is evaluated by the vacancy formation energy  $E_{\text{vac}}$ , which is derived from the following equation:

$$E_{\text{vac}} = E_{\gamma/\gamma'}^{\text{vac}} + \mu_{\text{Ni}} - E_{\gamma/\gamma'}. \quad (2)$$

Here,  $E_{\gamma/\gamma'}^{\text{vac}}$  and  $E_{\gamma/\gamma'}$  are total energies of the interface with and without vacancy, respectively. The second step is described by the migration barrier  $E_{\text{mig}}$ , which can be obtained from CI-NEB calculations. In this work, the diffusion activation energy  $E_Q$ , which presents the minimal energy needed to promote the diffusion process, is adopted to evaluate the effects of alloying elements on vacancy diffusion. It can be obtained by the following equation:

$$E_Q = E_{\text{vac}} + E_{\text{mig}}. \quad (3)$$

Considering the site preference of alloying elements within the interface region, to further investigate the effects of alloying on vacancy diffusion, we focus on the alloyed interface with the alloying elements at their favored Al-1 site and Ni-5 site, respectively. Since solute atoms have the greatest effects on their neighboring

sites, here we only consider the diffusion within three adjacent atomic layers of the substitutional site.

We first discuss the migration of Ni-vacancy from atomic layer  $-1$  to  $2$ , with solute atoms at their most favored Al-1 site. The energetics of Ni-vacancy formation and diffusion in the pure interface region are plotted in Fig. 2(a). As this figure shows, Ni-vacancy is more likely to form at layer 1, with the lowest  $E_{vac}$  among the three atomic layers, which equals to 1.41 eV. Besides,  $E_Q$  of the migration from atomic layer  $-1$  to  $1$  is 2.61 eV, slightly lower than that of the migration from layer 1 to  $2$ , indicating that the former process is more likely to occur. Based on the same method, we obtained the minimal  $E_{vac}$  and  $E_Q$  during the migration from atomic layer  $-1$  to  $2$  in the alloyed interfaces, as shown in Fig. 2(b). The black and red horizontal dashed lines represent the corresponding minimal energies in the pure interface region. The detailed energy values are provided in Table S1 in the supplementary material.

It can be observed in Fig. 2(b) that the variation of  $E_{vac}$  is smaller compared to  $E_Q$  upon the introduction of alloying elements, indicating that alloying elements have larger influence on  $E_{mig}$  than on  $E_{vac}$ . Among the seven alloying elements, Cr, Re, and W shift the vacancy formation energy most. As for the diffusion activation energy of Ni-vacancy, it has the sequence as  $Ta > W > Mo > Re > Ru > Cr > Al > Co$ . Since higher vacancy diffusion activation energy represents better resistance to creep deformation,<sup>46–48</sup> our calculations indicate that the substitution of Al-1 with the above alloying elements except for Co could retard the creep deformation process of superalloys. Moreover, Ta brings the best effect.

Besides, the diffusion behaviors of Ni-vacancy from atomic layer  $-3$  to  $-1$  with and without alloying elements substituted at the Ni-5 site are demonstrated in Fig. 3. The specific energy values

are provided in Table S2 in the supplementary material. It can be found in Fig. 3(a) that in the pure Ni/Ni<sub>3</sub>Al interface, Ni-vacancy is more likely to form at atomic layer  $-3$  and the migration process from layer  $-3$  to  $-2$  is easier to occur. As for the diffusion in alloyed interfaces with alloying elements at Ni-5 sites, the minimal  $E_{vac}$  and  $E_Q$  are illustrated in Fig. 3(b). Similar to the substitution at the Al-1 site, the effects of alloying elements at the Ni-5 site on vacancy migration energy are larger than that on vacancy formation energy. Interestingly, all alloying elements can promote the vacancy diffusion activation energies, and the magnitude of the promotion has a sequence of  $Ta > W > Mo > Re > Ru > Cr > Co > Ni$ , which is almost the same as that of the substitution at the Al-1 site. Besides, all seven alloying elements except for Ta tend to unfavor the formation of vacancy at their neighboring sites.

Our results reveal that Ta, W, Mo, Re, Ru, and Cr have better hindering effects on Ni-vacancy diffusion than the host atoms, no matter they are at the Al-1 site or Ni-5 site. These elements are believed to have good retarding effects on dislocation movements in the  $\gamma/\gamma'$  interface region, which would be beneficial to improve the creep deformation resistance of superalloys and further extend their service lifetime. Among them, Ta and W have the best effects from the viewpoint of diffusion activation energy, while the effect of Co is the weakest. By comparing Figs. 2(b) and 3(b), we can further find that alloying at the Al-1 site brings better retarding effects than alloying at the Ni-5 site.

### C. Alloying effects on the interface rupture strength

Since the rupture strength of the interface region reflects the rupture strength of superalloys to some extent, it is of interest to

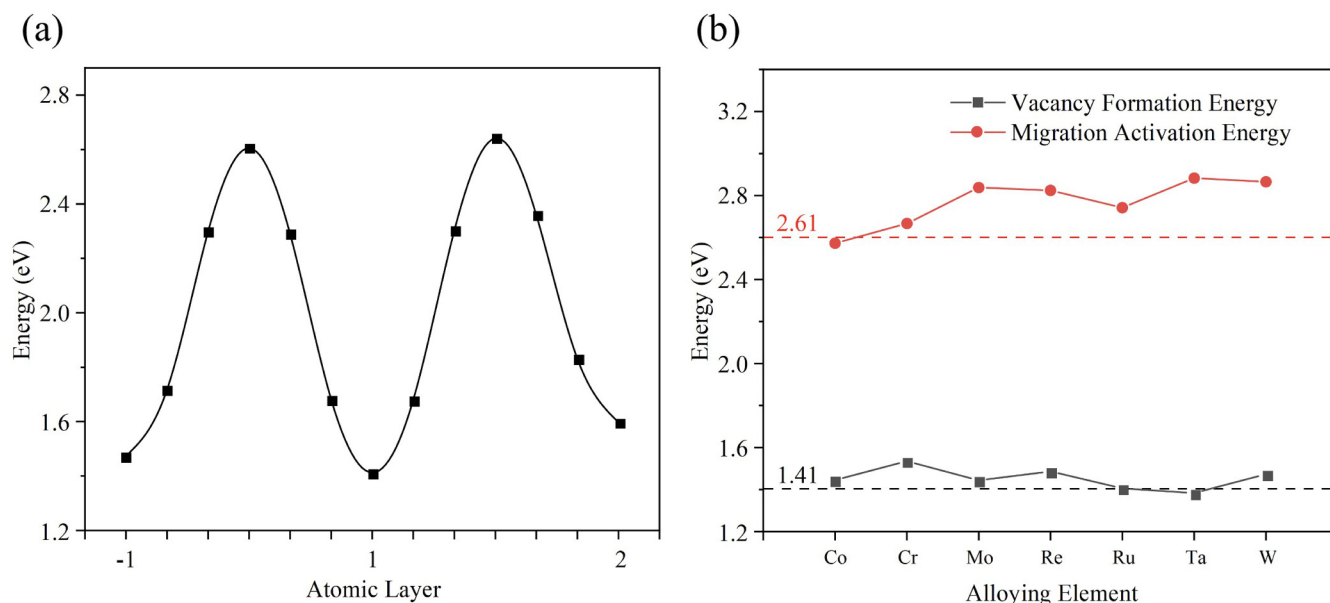


**FIG. 2.** (a) The energetics of Ni-vacancy formation and diffusion from atomic layer  $-1$  to  $2$  in a pure Ni/Ni<sub>3</sub>Al interface; (b) The minimal vacancy formation energy  $E_{vac}$  and migration activation energy  $E_Q$  during the diffusion around solute atoms at the Al-1 site.

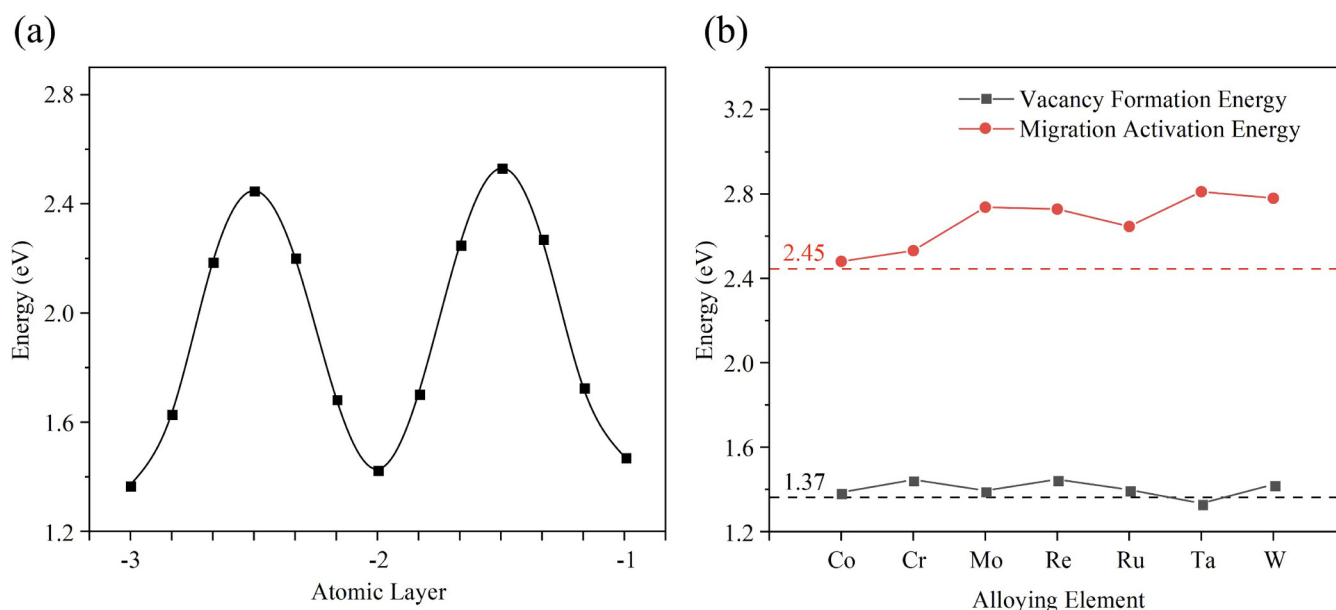


FIG. 3. (a) The energetics of Ni-vacancy formation and diffusion from atomic layer -3 to -1; (b) The minimal vacancy formation energy  $E_{vac}$  and migration activation energy  $E_Q$  during the diffusion around solute atoms at the Ni-5 site.

evaluate the effects of alloying elements on the rupture strength of the  $\gamma/\gamma'$  interface. The Griffith rupture work  $G$ , which is defined as the work needed to separate a crystal along the interface into two free surfaces,<sup>49</sup> is employed to evaluate the rupture strength of the

$\gamma/\gamma'$  interface region. It is derived from

$$G = (E_{\gamma}^{slab} + E_{\gamma'}^{slab} - E_{\gamma/\gamma'})/A, \quad (4)$$

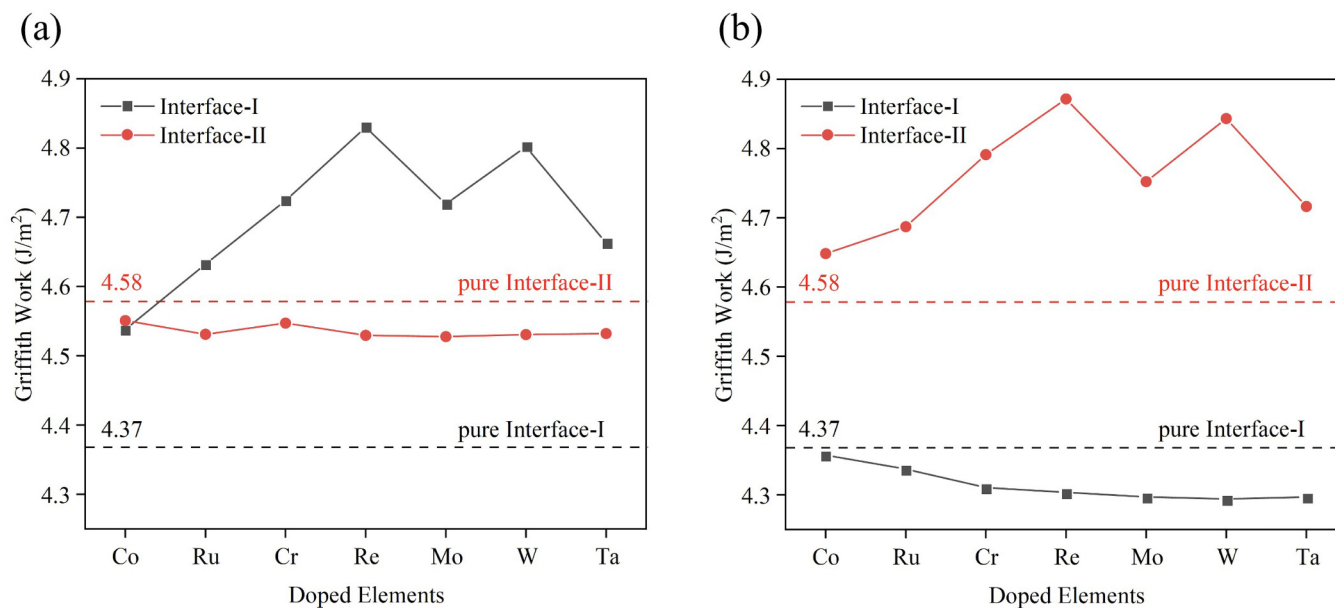


FIG. 4. The Griffith work of interface-I and interface-II when alloying elements locate at (a) Al-1 site; (b) Ni-5 site.

where  $E_{\gamma}^{slab}$ ,  $E_{\gamma'}^{slab}$ , and  $E_{\gamma/\gamma'}$  are the total energies of  $\gamma$  slab,  $\gamma'$  slab, and  $\gamma/\gamma'$  interface model, respectively.  $A$  denotes the area of coherent interface in the Ni/Ni<sub>3</sub>Al interface model as well as surface after cleavage. A more positive Griffith rupture work indicates that a larger force or energy is required to cleave the coherent interface, representing a higher rupture strength of the superalloy.

As shown in Fig. 1(a), there exist two potential fracture planes in the  $\gamma/\gamma'$  interface region. We will discuss the Griffith work of both interface-I and interface-II with the seven alloying elements at their favored Al-1 and Ni-5 sites, as illustrated in Fig. 4. The black and red horizontal dashed lines in Figs. 4(a) and 4(b) represent the Griffith work of pure interface-I and pure interface-II, respectively. The results show that it requires more energy to separate at interface-II than at interface-I for the pure Ni/Ni<sub>3</sub>Al interface,

indicating the stronger rupture strength of interface-II, which is in accordance with previous research studies.<sup>16,20</sup> It is worth mentioning that solutes at the horizontal axis in Fig. 4 are sorted according to their substitutional formation energies. Elements at the right side have lower substitutional energies, representing a more stable alloyed interface.

After we substituted alloying elements at their most favored Al-1 site in the interface region, the Griffith works of interface-I were promoted considerably [see Fig. 4(a)]. Meanwhile, the values of interface-II decreased a little bit. As a result, interface-II becomes the weaker plane in the interface region and limits the rupture strength of superalloy. However, the weaker fracture plane interface-II in the alloyed  $\gamma/\gamma'$  interface region still gets higher Griffith work than interface-I in the pure  $\gamma/\gamma'$  interface region,

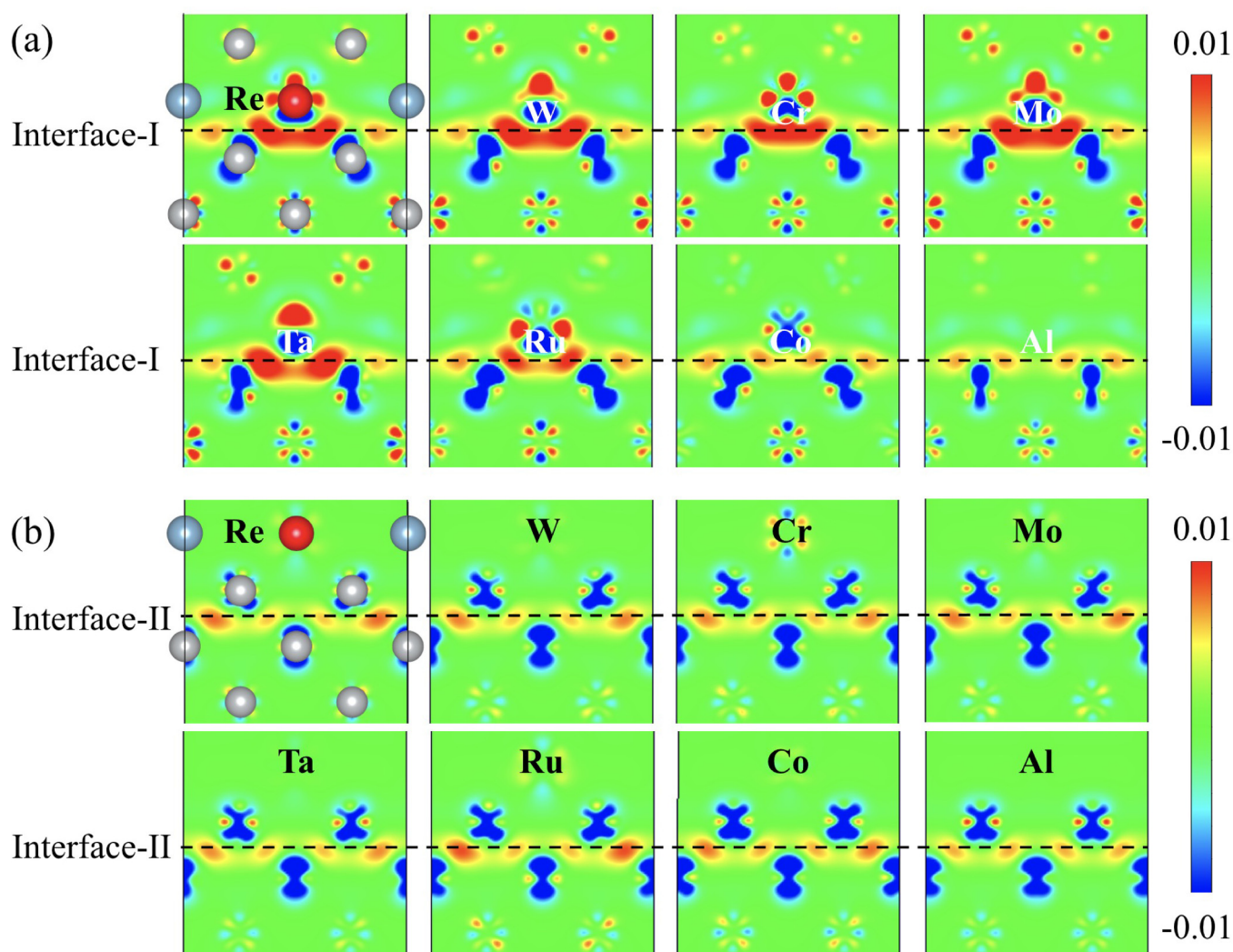


**FIG. 5.** The charge density difference diagrams of (a) interface-I and (b) interface-II when solutes are alloyed at the Al-1 site. The 2D images are sliced at the (020) plane, with the blue and gray balls denoting Al and Ni atoms, respectively. The solute atoms at the Al-1 site are signified by the red ball.

indicating all the seven alloying elements at the Al-1 site can improve the rupture strength of superalloys.

The strengthening tendency of alloying elements at the Al-1 site on their neighboring interface-I is in line with the result of Gong *et al.*<sup>21</sup> Among seven alloying elements, Re and W introduce the best strengthening effects. Meanwhile, the impacts of seven alloying elements on interface-II is relatively small and very similar.

As for the substitution at the Ni-5 site, the presence of alloying elements improves the rupture strength of interface-II and reduces that of interface-I. Since interface-I is already the weaker fracture plane in the pure interface, the results demonstrate that the alloying at the Ni-5 site would reduce the rupture strength of the  $\gamma/\gamma'$  interface region. Similar to the substitution at the Al-1 site, Re and W bring the best strengthening effect on their neighboring fracture plane interface-II. At the same time, Co and Ru reduce the rupture strength of interface-I by the smallest amount, W and Ta by the largest.

It is interesting to find that these solute atoms can always improve the rupture strength of their neighboring interface and reduce the rupture strength of their next neighboring interface. Moreover, there is a sequence of the strengthening effect introduced by solutes on the neighboring interface as  $\text{Re} > \text{W} > \text{Cr} > \text{Mo} > \text{Ta} > \text{Ru} > \text{Co}$ , no matter the solutes are located at the Al-1 site or Ni-5 site. Our results are generally consistent with those in experiments,<sup>1</sup> where the improvement in creep strength by alloying elements follow an order of  $\text{Re} > \text{W} > \text{Ta} > \text{Cr} > \text{Co}$ .

To get a more thorough understanding of the results, electronic structure analysis is conducted as well. We aim to figure out the origin of various strengthening effects among different alloying elements and their different effects on two potential fracture interfaces by looking at the charge density difference and hence the charge transfer between atoms.

Here, we take the substitution at the Al-1 site for discussions, which is the most favored sites for all seven solute elements to substitute. The charge density difference diagrams of interface-I and interface-II are depicted as Figs. 5(a) and 5(b), respectively. Part of the atomic layer is illustrated at the same time. From the reference bars in Fig. 5, we know that the deep blue represents charge depletion, while the deep red denotes electron accumulation. The result suggests an obvious charge accumulation at the objective interface, indicating the promotion of bonding between the atomic layers.

As shown in Fig. 5(a), the charge accumulation of interface-I due to the substitution of Re, W, Cr, and Mo is relatively close. However, a significant decrease of charge accumulation can be observed for Ta, Ru, Co, and Al, which is generally consistent with the strengthening effects of alloying elements on interface-I. Therefore, we consider the charge accumulation level between solute atoms and neighboring Ni atoms as one of the main factors determining the rupture strength of their neighboring interface.

In comparison with the charge accumulations around interface-I, the values of interface-II are quite similar and significantly smaller, suggesting that fewer electrons are transferred around interface-II. Meanwhile, as shown in Fig. 4(a), the Griffith works of interface-II are close and much lower than the values of interface-I. It can be found that the results of charge density differences are in good agreement with our discussion of the Griffith work. The above analysis reveals that the different effects of solute

atoms on their neighboring interface and next-neighboring interface originate from the different degree of charge accumulations.

#### IV. CONCLUSION

In this work, the alloying of the most common solute elements including Co, Cr, Mo, Re, Ru, Ta, and W in superalloys are systematically studied by first-principles calculations. Their effects on the Ni-vacancy diffusion behavior and the rupture strength of two potential fracture planes in the  $\gamma/\gamma'$  interface region are evaluated and analyzed. Our research has revealed that:

- (1) The site preference of seven solutes in the  $\gamma/\gamma'$  interface region follows the sequence of Al-1 > Ni-5 > Ni-4 > Ni-3 > Ni-1 > Ni-2 in general, except for Ru and Co, which prefer the Ni-2 site over the Ni-1 site.
- (2) The substitution of these solutes except for Co could significantly increase the barrier of Ni-vacancy diffusing within the  $\gamma/\gamma'$  interface region. The retarding effects are similar when solutes are located at their favored Al site and Ni site, which follow a sequence as  $\text{Ta} > \text{W} > \text{Mo} > \text{Re} > \text{Ru} > \text{Cr} > \text{Co}$ .
- (3) Alloying elements could always promote the rupture strength of their neighboring interface while decreasing that of their next neighboring interface.
- (4) The best strengthening effects on the neighboring interface are achieved by Re and W. In terms of the entire interface region, doping at the favored Al site brings a better strengthening effect than at the favored Ni site.
- (5) The charge accumulation degree between adjacent atomic layers decides the strengthening effect of alloying elements on the neighboring interface and explains the different rupture strength among two potential fracture planes.

#### SUPPLEMENTARY MATERIAL

See the [supplementary material](#) for details of the vacancy formation energy and diffusion activation energy of Ni-vacancy diffusion around solute atoms at the Al-1 site and Ni-5 site, respectively.

#### ACKNOWLEDGEMENTS

We gratefully acknowledge financial support provided by the National Key Research and Development Program of China (No. 2017YFB0701501) and Guangdong Province Key Area R&D Program (No. 2019B010940001). The computing facility from the  $\pi$  cluster at the Shanghai Jiao Tong University is also acknowledged.

#### DATA AVAILABILITY

The data that support the findings of this study are available from the corresponding author upon reasonable request.

#### REFERENCES

- <sup>1</sup>R. C. Reed, *The Superalloys: Fundamentals and Applications* (Cambridge University Press, Cambridge, 2006).
- <sup>2</sup>T. M. Pollock and S. Tin, "Nickel-based superalloys for advanced turbine engines: Chemistry, microstructure and properties," *J. Propul. Power* **22**, 361–374 (2006).



- <sup>3</sup>J.-C. Zhao and J. H. Westbrook, "Ultra-high-temperature materials for jet engines," *MRS Bull.* **28**, 622–630 (2003).
- <sup>4</sup>Z. Zhu, H. Basoalto, N. Warnken, and R. C. Reed, "A model for the creep deformation behaviour of nickel-based single crystal superalloys," *Acta Mater.* **60**, 4888–4900 (2012).
- <sup>5</sup>T. Sugui, Z. Jinghua, Z. Huihua, Y. Hongcai, X. Yongbo, and H. Zhuangqi, "Aspects of primary creep of a single crystal nickel-base superalloy," *Mater. Sci. Eng. A* **262**, 271–278 (1999).
- <sup>6</sup>F. Mompou and D. Caillard, "Dislocation-climb plasticity: Modelling and comparison with the mechanical properties of icosahedral AlPdMn," *Acta Mater.* **56**, 2262–2271 (2008).
- <sup>7</sup>H. J. Frost and M. F. Ashby, *Deformation Mechanism Maps the Plasticity and Creep of Metals and Ceramics* (Pergamon Press, Oxford, 1998).
- <sup>8</sup>X. G. Wang, J. L. Liu, T. Jin, X. F. Sun, Y. Z. Zhou, Z. Q. Hu, J. H. Do, B. G. Choi, I. S. Kim, and C. Y. Jo, "Creep deformation related to dislocations cutting the  $\gamma'$  phase of a Ni-base single crystal superalloy," *Mater. Sci. Eng. A* **626**, 406–414 (2015).
- <sup>9</sup>Y. Ru, H. Zhang, Y. Pei, S. Li, and S. Gong, "Substituting Mo for Re in equal weight for Ni based single crystal superalloy," *Materialia* **6**, 100278 (2019).
- <sup>10</sup>Y. Ru, S. Li, J. Zhou, Y. Pei, H. Wang, S. Gong, and H. Xu, "Dislocation network with pair-coupling structure in  $\{111\}$   $\gamma/\gamma'$  interface of Ni-based single crystal superalloy," *Sci. Rep.* **6**, 29941 (2016).
- <sup>11</sup>X. Zhang, Y. Li, J. Tang, L. Deng, W. Li, L. Wang, H. Deng, and W. Hu, "Precipitate/vanadium interface and its strengthening on the vanadium alloys: A first-principles study," *J. Nucl. Mater.* **527**, 151821 (2019).
- <sup>12</sup>X. Lv and J. Zhang, "Core structure of  $a\sqrt{2}\langle 100 \rangle$  interfacial superdislocations in a nickel-base superalloy during high-temperature and low-stress creep," *Mater. Sci. Eng. A* **683**, 9–14 (2017).
- <sup>13</sup>Y. Gao and A. C. F. Cocks, "Thermodynamic variational approach for climb of an edge dislocation," *Acta Mech. Solida Sin.* **22**, 426–435 (2009).
- <sup>14</sup>F. R. N. Nabarro, "Steady-state diffusional creep," *Philos. Mag.* **16**, 231–237 (1967).
- <sup>15</sup>P. Peng, Z. H. Jin, R. Yang, and Z. Q. Hu, "First principles study of effect of lattice misfit on the bonding strength of Ni/Ni<sub>3</sub>Al interface," *J. Mater. Sci.* **39**, 3957–3963 (2004).
- <sup>16</sup>P. Peng, A. K. Soh, R. Yang, and Z. Q. Hu, "First-principles study of alloying effect of Re on properties of Ni/Ni<sub>3</sub>Al interface," *Comput. Mater. Sci.* **38**, 354–361 (2006).
- <sup>17</sup>S. G. Tian, Z. G. Guo, D. L. Shu, and J. Xie, "Damage and fracture mechanism of a nickel-based single crystal superalloy during creep at moderate temperature," *Mater. Sci. Forum* **783–786**, 1188–1194 (2014).
- <sup>18</sup>M. Sun, Z. Li, G.-Z. Zhu, W.-Q. Liu, S.-H. Liu, and C.-Y. Wang, "Diffusion in Ni-based single crystal superalloys with density functional theory and kinetic Monte Carlo method," *Commun. Comput. Phys.* **20**, 603–618 (2016).
- <sup>19</sup>M. Sun and C.-Y. Wang, "First principles study of the diffusional phenomena across the clean and Re-doped  $\gamma$ -Ni/ $\gamma'$ -Ni<sub>3</sub>Al interface of Ni-based single crystal superalloy," *Chin. Phys. B* **25**, 067104 (2016).
- <sup>20</sup>W. Zhao, Z. Sun, and S. Gong, "Vacancy mediated alloying strengthening effects on  $\gamma/\gamma'$  interface of Ni-based single crystal superalloys: A first-principles study," *Acta Mater.* **135**, 25–34 (2017).
- <sup>21</sup>X.-F. Gong, G. X. Yang, Y. H. Fu, Y. Q. Xie, J. Zhuang, and X.-J. Ning, "First-principles study of Ni/Ni<sub>3</sub>Al interface strengthening by alloying elements," *Comput. Mater. Sci.* **47**, 320–325 (2009).
- <sup>22</sup>S. H. Liu, C. P. Liu, W. Q. Liu, X. N. Zhang, P. Yan, and C. Y. Wang, "Investigation of the elemental partitioning behaviour and site preference in ternary model nickel-based superalloys by atom probe tomography and first-principles calculations," *Philos. Mag.* **96**, 2204–2218 (2016).
- <sup>23</sup>C. Zhu, T. Yu, C. Wang, and D. Wang, "First-principles study of Ni/Ni<sub>3</sub>Al interface doped with Re, Ta and W," *Comput. Mater. Sci.* **175**, 109586 (2020).
- <sup>24</sup>Q. Feng, L. J. Carroll, and T. M. Pollock, "Solidification segregation in ruthenium-containing nickel-base superalloys," *Metall. Mater. Trans. A* **37**, 1949–1962 (2006).
- <sup>25</sup>H. Harada, A. Ishida, Y. Murakami, H. K. D. H. Bhadeshia, and M. Yamazaki, "Atom-probe microanalysis of a nickel-base single crystal superalloy," *Appl. Surf. Sci.* **67**, 299–304 (1993).
- <sup>26</sup>R. C. Reed, A. C. Yeh, S. Tin, S. S. Babu, and M. K. Miller, "Identification of the partitioning characteristics of ruthenium in single crystal superalloys using atom probe tomography," *Scr. Mater.* **51**, 327–331 (2004).
- <sup>27</sup>R. Srinivasan, R. Banerjee, J. Y. Hwang, G. B. Viswanathan, J. Tiley, D. M. Dimiduk, and H. L. Fraser, "Atomic scale structure and chemical composition across order-disorder interfaces," *Phys. Rev. Lett.* **102**, 086101 (2009).
- <sup>28</sup>P. Hohenberg, W. Kohn, and I. E. Gas, *Phys. Rev.* **136**, B864–B871 (1964).
- <sup>29</sup>W. Kohn and L. J. Sham, "Self-consistent equations including exchange and correlation effects," *Phys. Rev.* **140**, A1133–A1138 (1965).
- <sup>30</sup>G. Kresse and J. Furthmüller, "Efficient iterative schemes for *ab initio* total-energy calculations using a plane-wave basis set," *Phys. Rev. B* **54**, 11169 (1996).
- <sup>31</sup>P. E. Blöchl, "Projector augmented-wave method," *Phys. Rev. B* **50**, 17953 (1994).
- <sup>32</sup>G. Kresse and D. Joubert, "From ultrasoft pseudopotentials to the projector augmented-wave method," *Phys. Rev. B* **57**, 1758 (1999).
- <sup>33</sup>J. P. Perdew, K. Burke, and M. Ernzerhof, "Generalized gradient approximation made simple," *Phys. Rev. Lett.* **77**, 3865 (1996).
- <sup>34</sup>G. Henkelman, B. P. Uberuaga, and H. Jónsson, "A climbing image nudged elastic band method for finding saddle points and minimum energy paths," *J. Chem. Phys.* **113**, 9901–9904 (2000).
- <sup>35</sup>Transition state tools for VASP, see <http://theory.cm.utexas.edu/vtsttools/index.html> for more information about transition state tools for VASP; accessed 1 July 2019.
- <sup>36</sup>Y. Zhou, Z. Mao, C. Booth-Morrison, and D. N. Seidman, "The partitioning and site preference of rhenium or ruthenium in model nickel-based superalloys: An atom-probe tomographic and first-principles study," *Appl. Phys. Lett.* **93**, 171905 (2008).
- <sup>37</sup>A. F. Kohan, G. Ceder, D. Morgan, and C. G. Van de Walle, "First-principles study of native point defects in ZnO," *Phys. Rev. B* **61**, 15019–15027 (2000).
- <sup>38</sup>X. Zhang and C.-Y. Wang, "First-principles study of vacancy formation and migration in clean and Re-doped  $\gamma'$ -Ni<sub>3</sub>Al," *Acta Mater.* **57**, 224–231 (2009).
- <sup>39</sup>D. Blavette, P. Caron, and T. Khan, "An atom probe investigation of the role of rhenium additions in improving creep resistance of Ni-base superalloys," *Scr. Metall.* **20**, 1395–1400 (1986).
- <sup>40</sup>N. Wanderka and U. Glatzel, "Chemical composition measurements of a nickel-base superalloy by atom probe field ion microscopy," *Mater. Sci. Eng. A* **203**, 69–74 (1995).
- <sup>41</sup>P. J. Warren, A. Cerezo, and G. D. W. Smith, "An atom probe study of the distribution of rhenium in a nickel-based superalloy," *Mater. Sci. Eng. A* **250**, 88–92 (1998).
- <sup>42</sup>M. Mantina, Y. Wang, R. Arroyave, L. Q. Chen, Z. K. Liu, and C. Wolverton, "First-principles calculation of self-diffusion coefficients," *Phys. Rev. Lett.* **100**, 215901 (2008).
- <sup>43</sup>N. L. Peterson, "Self-diffusion in pure metals," *J. Nucl. Mater.* **69–70**, 3–37 (1978).
- <sup>44</sup>J. R. Manning and L. J. Bruner, "Diffusion kinetics for atoms in crystals," *Am. J. Phys.* **36**, 922–923 (1968).
- <sup>45</sup>S. L. Shang, H. Z. Fang, J. Wang, C. P. Guo, Y. Wang, P. D. Jablonski, Y. Du, and Z. K. Liu, "Vacancy mechanism of oxygen diffusivity in bcc Fe: A first-principles study," *Corros. Sci.* **83**, 94–102 (2014).
- <sup>46</sup>M. Grabowski, J. Rogal, and R. Drautz, "Kinetic Monte Carlo simulations of vacancy diffusion in nondilute Ni-X (X = Re, W, Ta) alloys," *Phys. Rev. Mater.* **2**, 123403 (2018).
- <sup>47</sup>D. Mordehai, E. Clouet, M. Fivel, and M. Verdier, "Introducing dislocation climb by bulk diffusion in discrete dislocation dynamics," *Philos. Mag.* **88**, 899–925 (2008).
- <sup>48</sup>P. Wollgramm, H. Buck, K. Neuking, A. B. Parsa, S. Schuwallow, J. Rogal, R. Drautz, and G. Eggeler, "On the role of Re in the stress and temperature dependence of creep of Ni-base single crystal superalloys," *Mater. Sci. Eng. A* **628**, 382–395 (2015).
- <sup>49</sup>Q. M. Hu, R. Yang, D. S. Xu, Y. L. Hao, D. Li, and W. T. Wu, "Energetics and electronic structure of grain boundaries and surfaces of B- and H-doped Ni<sub>3</sub>Al," *Phys. Rev. B* **67**, 224203 (2003).